Electronic Supplementary Material (ESI) for Physical Chemistry Chemical Physics.

Supporting Information

Tuning of intrinsic antiferromagnetic to ferromagnetic ordering in microporous α-MnO_2 by inducing tensile strain

G.Kruthika[a,b], J.Karthikeyan[a,b], and P.Murugan[a,b]*

[a]Functional Materials Division, CSIR Central Electrochemical Research Institute (CECRI), Karaikudi−630 003, Tamil Nadu, India

[b]Academy of Scientific & Innovative Research, CECRI, India

*E-mail: murugan@cecri.res.in.

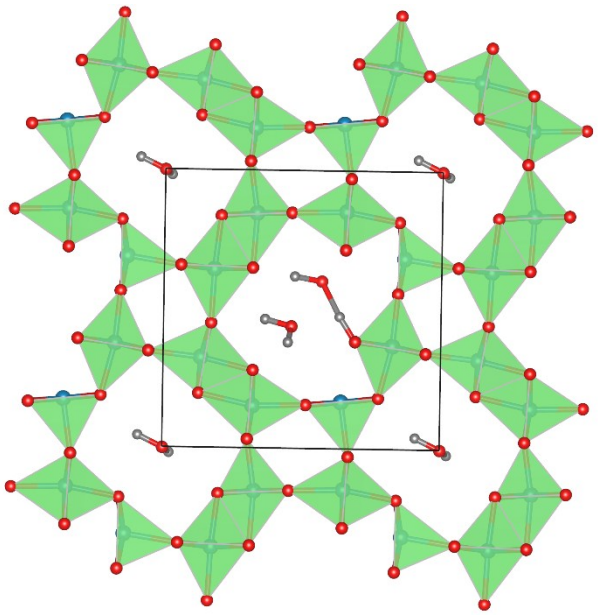

Fig. S1: Polyhedral model of optimized structure of α-MnO_2. $0.375H_2O$ compound. It is observed that the tunnel accommodated with two water molecules distorts the crystal structure. Thus, it gives lesser stability as compared to α-MnO_2. $0.25H_2O$ compound.

Table. S1. Number of sites obeying GKA rule (two Mn atoms that are connected through O(sp^2) atoms) and triangular (Δ) rule (in the double chain) in different types of magnetic configurations of α-MnO_2.0.25 H_2O.

Type	AFM-C	AFM-C2	AFM-A2	FM	FIM
Δ rule	All 4 sites are not obeyed	All 4 sites are obeyed	All 4 sites are not obeyed	All 4 sites are obeyed	All 4 sites are obeyed
GKA rule	All 4 sites are obeyed	All 4 sites are obeyed	All 4 sites are not obeyed	All 4 sites are not obeyed	Only 2 sites are obeyed

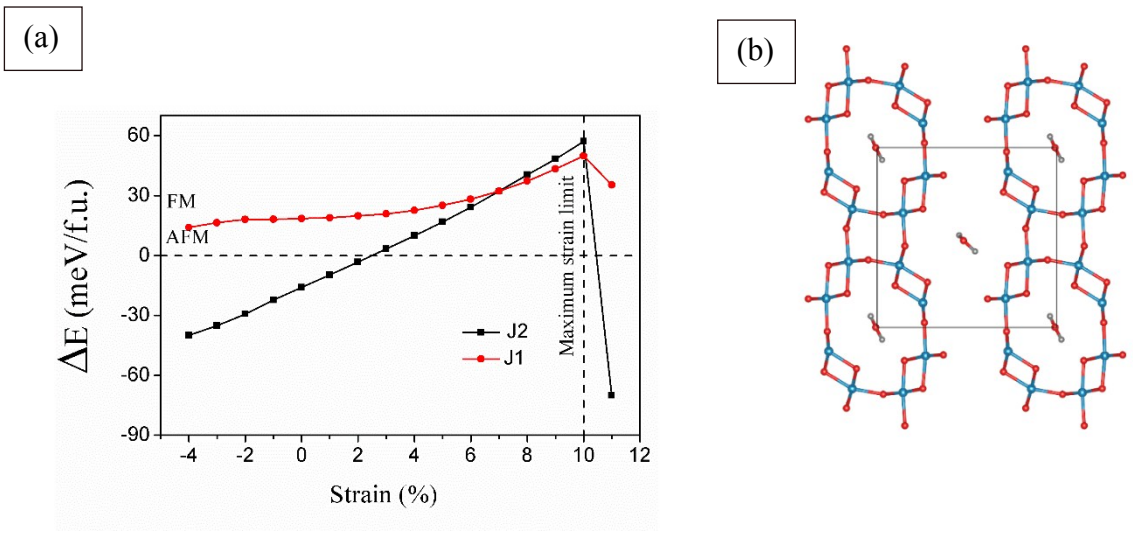

Fig. S2 (a). Exchange energies (J1, J2) are shown with respect to triaxial strain. (b) Optimized structure distorted at 11% tensile strained α-MnO_2.0.25H_2O. It is observed that at 11% tensile strain, the linkage between double chains is broken.

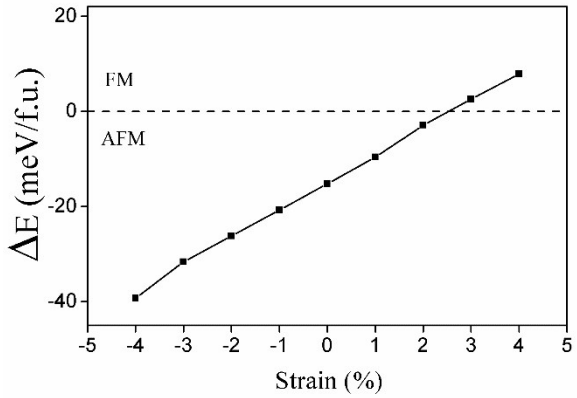

Fig. S3. Exchange energy (J2) for unhydrated α-MnO_2 compound. It shows that the FM ordering is induced by an application of 3% tensile strain.

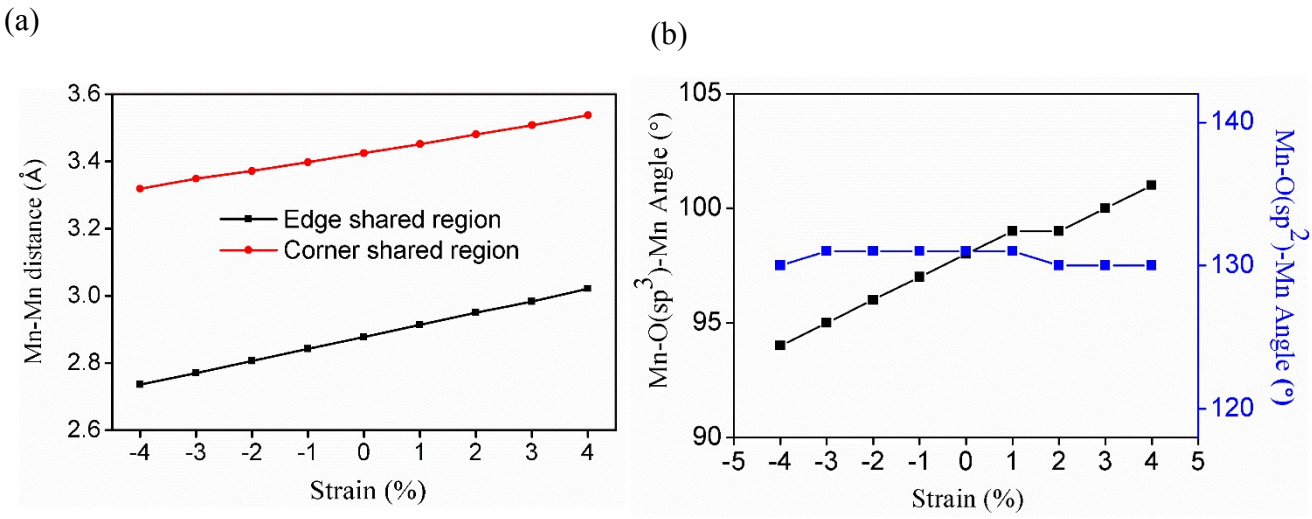

Fig. S4: Variation of (a) Mn-Mn distance and (b) Mn-O-Mn angle with respect to the triaxial strain introduced α-MnO_2.0.25H_2O compound. All the values are given for AFM-C2 configuration.

Table. S2. Comparison of various parameters of unstrained and 4% tensile strained α-MnO_2. 0.25H_2O compound, calculated using different exchange correlation functionals (PW91 and PBE).

		Unstrained	4% tensile strain
Moment on Mn atoms (μ_B)	PW91	3.2	3.4
	PBE	3.1	3.3
Exchange Energy ($\Delta = E_{afmc2\text{-}fm}$) (meV/f.u.)	PW91	-16	10
	PBE	-9	19

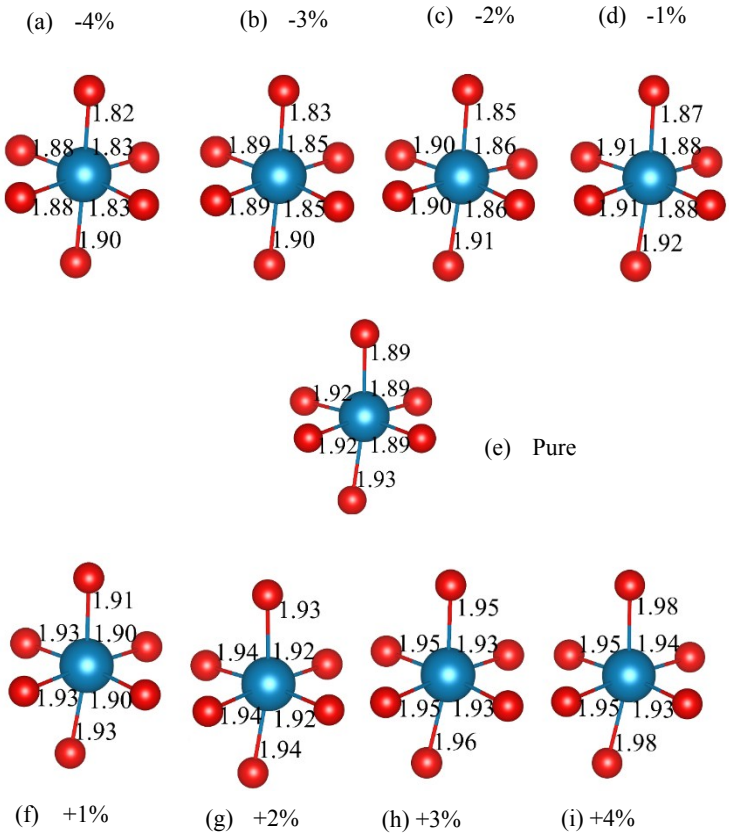

Fig. S5: The distortion in geometry of MnO_6 octahedra are shown for various triaxial strained α-MnO_2 compounds. Mn-O bond distances (in Å) are given in the diagram.

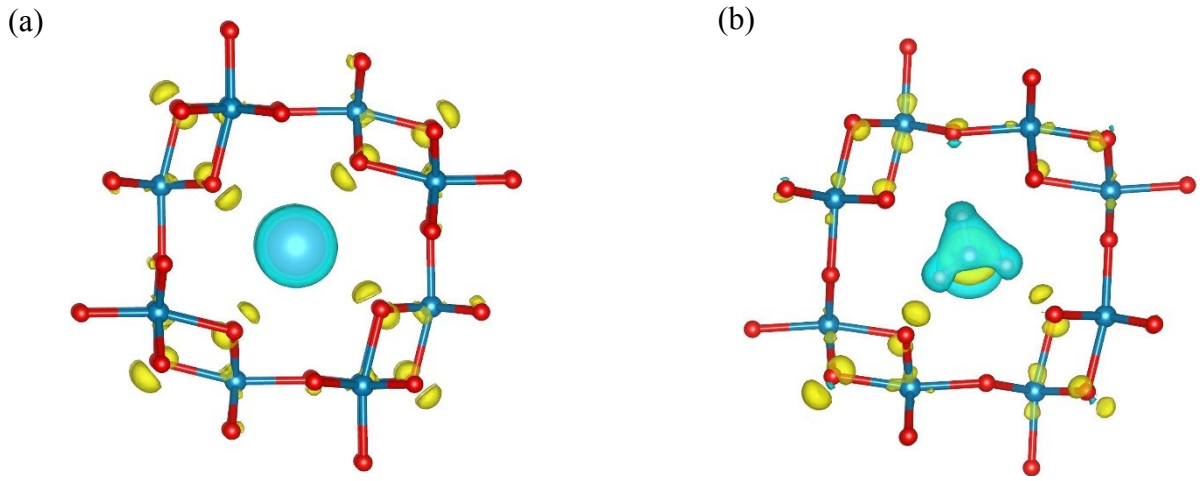

Fig. S6: Charge transfer between sorbent and α-MnO_2 framework ($\Delta\rho = \rho_{\alpha\text{-}MnO2\ .0.25X} - \rho_{\alpha\text{-}MnO2} - \rho_X$) is shown for α-$MnO_2$ .0.25X compound, where X = Xe (a) and NH_3 (b). It demonstrates that the small charge transfer is occurred between the tunnel species and lattice oxygen. Isosurface for respective compounds are plotted for values of 3×10^{-3} and 4×10^{-3} e/Å^3 respectively. Yellow (blue) isosurface represents charge accumulation (depletion) region.

Table. S3. Lattice parameters, relative energy of α-MnO_2 compound having various tunnel species with respect to different (AFM-C2, FM) magnetic configurations and local magnetic moment (absolute average value) of Mn, O(sp^3), O(sp^2) atoms in their stable ground state magnetic configurations.

Tunnel species	Lattice parameters (Å)			Magnetic configurations (meV/f.u.)		Local magnetic moment (μ_B)		
	a	b	c	AFM-C2	FM	Mn	O(sp^3)	O(sp^2)
Ar	9.83	9.83	2.90	0	12	3.2	0.2	0.0
Kr	9.86	9.87	2.92	0	8	3.3	0.2	0.0
Xe	9.99	9.99	2.96	28	0	3.4	0.2	0.1
NH_3	10.04	9.73	2.89	20	0	3.4	0.2	0.1
CH_4	9.69	9.89	2.90	0	13	3.2	0.2	0.0
H_2S	9.92	9.98	2.79	0	83	3.0	0.1	0.0
Li_2O	9.80	10.14	2.89	2	0	3.5	0.2	0.1